Polymer-Surfactant Films at the Air-Water Interface. 2. A Neutron Reflectivity Study

L. T. Lee,*,† E. K. Mann,‡ O. Guiselin,† D. Langevin,‡ B. Farnoux,† and J. Penfold§

Laboratoire Léon Brillouin, Laboratoire mixte CEA-CNRS, C.E. de Saclay, 91191 Gif/Yvette, France, Laboratoire de Physique Statistique de l'ENS, Associé aux Universités Paris VI et VII, 75231 Paris, France, and Rutherford Appleton Laboratory, Didcot, England

Received January 19, 1993; Revised Manuscript Received July 28, 1993®

ABSTRACT: Mixed polymer-surfactant films at the air-water interface have been studied using neutron reflectivity. When poly(dimethylsiloxane) is spread on the surface of a surfactant layer, the resultant mixed film is a superposition of two layers: one surfactant-rich and one polymer-rich. The composition and the degree of mixing of the layers depend on the nature of the surfactant. We find significant penetration of the polymer into a monolayer of single-chain nonionic surfactant, $C_{10}E_5$. For a double-chain anionic surfactant, AOT, no interpenetration of the two layers is detected. This difference is most probably due to the greater flexibility of the $C_{10}E_5$ monolayer compared to that of AOT. The higher degree of hydration of the nonionic surfactant layer could also play a role in the mixing behavior of the polymer and surfactant layers. The molecular thickness of the polymer layer indicates a flat two-dimensional conformation of the spread polymer. The results from this study together with those in part 1 our paper suggest that the wetting behavior of the polymer is related to the degree of interpenetration of the polymer and surfactant layers.

Introduction

Spread molecular layers of polymers on the surface of water have been widely studied[1-12] due to their numerous practical applications. Frequently, these spread polymer layers are insoluble in the bulk phase, thereby acting as efficient modifiers of interfacial properties including surface rheology. Most of the past studies have involved characterizations of surface pressure-area isotherms, and elasticities of the polymer films. Since these films are of molecular dimensions, it has not been until recently that structural information has been attainable using ellipsometry[5-7,9] and reflectivity techniques.[10,11] The principal question is whether, when deposited on a polar surface, the polymer molecule undergoes a change in conformation from its natural three-dimensional random coil to a spread out two-dimensional film. It has been noted that such a change in conformation depends not so much on the polarity of the molecule as the competition between monomer-monomer and monomer-surface interaction,[1,2] with the latter favoring a spread out conformation. In the case of poly(dimethylsiloxane) (PDMS) on water, hydrogen bonding between the oxygen of the siloxane backbone and the water molecules effect such a conformation. This hypothesis, dating back from early days,[13] was recently confirmed unequivocally using neutron reflectivity on PDMS of different chain lengths.[10]

In the present case, we extend our study to a three component system: the PDMS is spread on a surfactant solution, the surface of which is covered with a surfactant monolayer. Two important questions we would like to address are (i) what is the conformation of the spread polymer and (ii) will the polymer mix with this surfactant layer or will it form a separate layer on top of the initial surfactant layer or will it follow an intermediate route, i.e., penetrate partially the surfactant layer but with its center of mass remaining on top of the surfactant layer. This second problem has already been addressed in the literature for the case of alkanes. It is generally agreed upon, from existing experimental data,[14-16] that when the alkane chain length is smaller than that of the surfactant chain, the oil molecules penetrate the surfactant layer, whereas for longer alkane chains, no penetration occurs. This problem is currently being studied by Thomas and co-workers.[17] In the case of polymers, which are long molecules, one would expect little penetration. However, for the case of PDMS, the Si-O group can interact with the surface and may thus favor mixing with the surfactant molecules. Surface pressure and ellipsometry experiments and Brewster angle microscopy have been carried out on PDMS-surfactant systems and are described in part 1[18] of this paper. The results strongly suggest the existence of two separate surfactant and polymer layers, but interpenetration of the layers cannot be explored using these techniques. Neutron reflectivity is an ideal tool to investigate this problem due to the high spatial resolution as well as the possibility of varying contrast between the two layers and the subtrate by selective deuteration.

Experimental Methods

Neutron reflectivity experiments were performed on the time-of-flight reflectometer, CRISP, at the Rutherford Appleton Laboratory (Spallation Source). The incident angle was 1.5° with an angular resolution of 8%. A large spectrum of neutron wavelength from 0.7 to 10.5 Å was obtained by running the chopper at 25 Hz.

The polymer sample, a fully deuterated PDMS (M_w = 84 000; M_w/M_n = 1.29) was prepared and characterized by A. Lapp (Saclay). Two surfactant solutions were investigated, an anionic double-chain surfactant, aerosol OT (AOT) and a nonionic single-chain surfactant, penta(ethylene glycol) mono-*n*-decyl ether ($C_{10}E_5$). The bulk concentrations were about 3 times the cmc to ensure the presence of a saturated monolayer of surfactant on the surface. Two isotopic subphases were used: 100% D_2O and an air contrast-matched water. The polymer was spread on the surface of the surfactant solution using *n*-hexane as the spreading agent. The surface concentration of polymer was increased by successive addition to a constant surface area.

The sample cell (100 × 40 × 2 mm), made of aluminum, was enclosed in a quartz cell to minimize evaporation of the subphase. The data acquisition time for each sample was about 3 h for the D_2O subphase and about 7-8 h for the air contrast-matched water subphase.

† Laboratoire Léon Brillouin.
‡ Ecole Normale Supérieure.
§ Rutherford Appleton Laboratory.
® Abstract published in *Advance ACS Abstracts*, October 15, 1993.

0024-9297/93/2226-7046$04.00/0

Results and Discussion

The propagation of thermal neutrons is analogous to that of electromagnetic radiation in the s polarization. Therefore classical optical phenomena such as reflection, refraction, and interference are also observed with neutrons. Descriptions of neutron optics and theoretical treatments of neutron reflectivity[19] as well as the numerous applications of the technique[20] can be found elsewhere in the literature. Neutron reflectivity from a surface depends on the component of the wave vector, k_z, normal to the surface. k_z is defined as $(2\pi/\lambda)\sin\theta$ where λ is the neutron wavelength and θ is the grazing incident angle of the neutron beam with respect to the surface. In a neutron reflectivity experiment, one measures the reflectivity R, defined as the ratio of the intensities of specularly reflected beam and direct beam, as a function of k_z (or wave vector transfer Q). In this paper, we report our reflectivity as a function of k_z. The neutron refractive index, n, of a medium neglecting absorption is defined as[19]

$$n = 1 - \frac{Nb}{2\pi}\lambda^2$$

Nb is the average coherent scattering length density of the medium. For a perfect interface, void of structure and roughness, the refractive index changes abruptly as a step function from one material to another, and one obtains the classical Fresnel reflectivity.[21] Such an interface is never encountered in real systems. Deviations from the Fresnel reflectivity arise from surface imperfections such as those due to adsorption or surface roughness. In specular reflection, these deviations are related to inhomogeneities perpendicular to the reflecting surface and can be used to deduce concentration profiles of the refractive index (and therefore the structure and composition of interfacial layers) perpendicular to the surface. However, one has to take into account possible effects of diffuse scattering even though the reflectivity measurements are performed under specular conditions. Diffuse scattering can arise from in-plane surface inhomogeneities or from bulk scattering objects close to the surface. These effects show up as "shoulders" on the specular reflection peak and should be subtracted from the specular peak. In this case, even though one takes care of an important part of diffuse scattering effects, some doubt still remains as to whether the correct amount of subtraction has been made.

In our experiments, we have performed independent measurements on a few of our samples using a multidetector. In all cases, the specular reflection peaks show normal distributions without any "shoulders". Although it is not possible to claim from these data that diffuse scattering effects are completely absent, we have considered them to be insignificant.

Note that although quantitative information on in-plane inhomogeneity is not easily accessible by neutron specular reflection, X-ray reflectivity and scattering measurements have been performed to obtain such information on surfaces of solid glass,[22] liquids[23–25] and polymer systems.[26] With neutrons, due to the much lower flux and the smaller coherence lengths compared to X-rays, off-specular reflection measurements are more difficult to perform and the sensitivity to in-plane inhomogeneity significantly reduced.

In this paper, we present results of specular neutron reflection from mixed polymer–surfactant layers on the surface of an aqueous substrate. The optical matrix method[21,27,28] is used to analyze the reflectivity data. In this method, the surface region is divided into successive discrete layers with constant refractive indices. An iterative calculation of the reflection and transmission coefficients at each interface yields the total reflectivity. The calculated model curve is then compared with the experimental curve. The goodness of fit and acceptance of a model are determined by the χ^2 values. Due to the rapidly increasing number of parameters one encounters as the number of surface layers increases, some physically reasonable assumptions can make the data analysis much less tedious (in our case, we assume the surfactant layer thickness to remain constant in the presence of polymers).

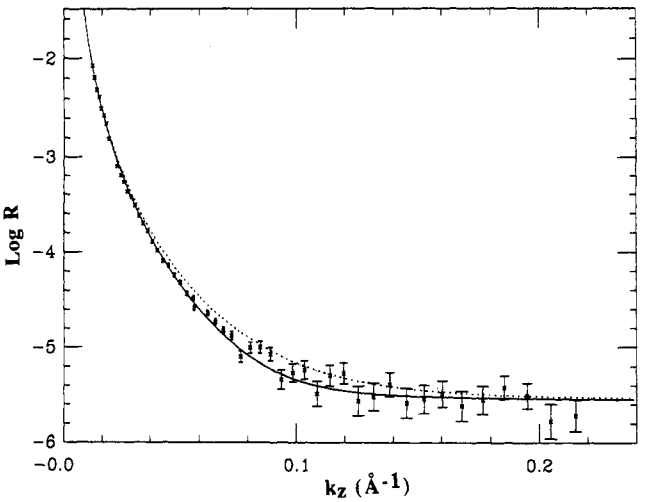

Figure 1. Reflectivity curve of AOT in D_2O. The dotted line is the Fresnel curve; the continuous line is calculated using a one-layer model: d_s = 13 Å, Nb = 0.90E-6 Å^{-2}.

Neutron reflectivity measurements of adsorbed semidilute polymer layers, or of moderately dense organic surface layers of molecular dimensions, often give rise to monotonic reflectivity curves void of any special features. Interpretations of such curves can be tricky and in order to obtain unique solutions to these curves, data of several isotopic contrasts coupled with physically reasonable hypotheses and theoretical models are required. Such an approach has been successfully applied to the study of surfactant monolayers[29,30] and concentration profiles of polymer layers[31–33] adsorbed from solution at the liquid–air and solid–liquid interface.

In the present study of an insoluble polymer deposited on a surfactant layer, we have chosen a combination of relative contrast in the neutron refractive indices of the system components such that the structural features of a reflectivity curve are enhanced. This consists of a layer of protonated surfactant sandwiched between deuterated polymer and deuterated subphase. The maximum contrast in refractive indices at each interface thus augments the interference effects in the reflectivity. Air contrast-matched water is also used as a subphase to deduce the extent of inclusion of water molecules in the surface layers.

Figure 1 shows the reflectivity curve (log R versus k_z) of the surface of AOT solution in D_2O. The deviation of the reflectivity from the Fresnel curve (dotted line) is due to the presence of the surfactant monolayer. The structures of surfactant monolayers have been studied in great detail using X-ray[34] and neutron reflectivity.[29,30] Our purpose here is not to concentrate on the detailed features of the surfactant layer but to study the behavior of spread polymer layers on the surfactant. Therefore, for the purpose of simplicity, the reflectivity curve of the AOT monolayer has been fitted to a one-layer model (continuous line). We find a good agreement between the experimental

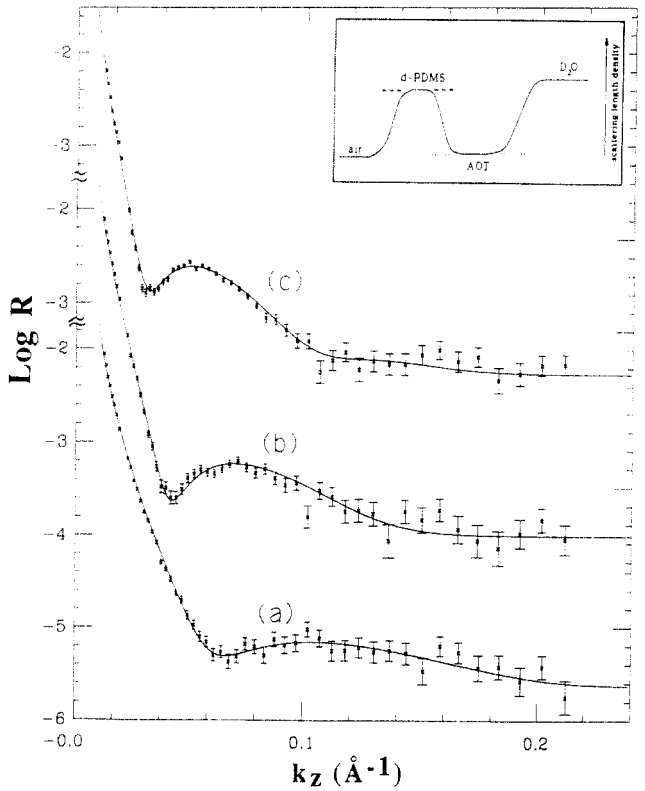

Figure 2. Reflectivity data for deuterated PDMS on the AOT monolayer with D_2O as the subphase at different polymer surface concentrations: 1 monolayer (a); 2 monolayers (b); 3 monolayers (c). The continuous lines are calculated using a two-layer model with the density profile shown in the inset (scattering length density for pure polymer (dashed line), for pure surfactant (dotted line)).

data and the calculated curve using an overall thickness d_s = 13 Å and an average neutron scattering length density Nb = 0.90E-6 Å^{-2}. The scattering length density obtained in this case is higher than that of the average for pure AOT (Nb = 0.59E-6 Å^{-2}), which can only be due to inclusion of D_2O (Nb = 6.39E-6 Å^{-2}) in the layer. Assuming the surfactant layer to be composed of surfactant molecules and D_2O, we deduce the volume fraction of surfactant ϕ_s = 0.95 and volume fraction of water ϕ_w = 0.05. A value of 9 Å is introduced as the width of the water–surfactant interface and 5 Å as the surfactant–air interface. The interfacial width is defined as the distance between two media; in the presence of a layer, the average of the widths of its two interfaces should be equal to or less than the layer thickness. The width of this interface takes into account, to a certain extent, thermally induced roughness. In our case, we have described the interface by a polynomial function to the fifth order but a simpler function can also be used.

When the equivalent of one monolayer of deuterated PDMS (C_p = 0.8 mg/m^2, which is the concentration where monomer steric repulsions are felt; it is also interpreted as the transition region between dilute and semidilute regimes in two dimensions[35]) is added to the AOT covered surface, the reflectivity curve (Figure 2a) exhibits interference features. In this case, it is not possible to fit the data using a one-layer model. This suggests that the polymer does not penetrate the surfactant layer to form a homogeneously mixed polymer–surfactant film. However, a good fit is obtained using a two-layer model which consists of a surfactant-rich and a polymer-rich layer. In this model, we have imposed the constraint that the overall thickness of the surfactant layer remained constant; the scattering length density, however, is allowed to vary. The continuous line is calculated using the following parameters: for the AOT-rich layer, d_s = 13 Å and Nb = 0.90E-6 Å^{-2}; for the polymer-rich layer, d_p = 6.5 Å and Nb = 4.95E-6 Å^{-2} (Nb = 5.01E-6 Å^{-2} for pure deuterated PDMS). Note that the average scattering length density of the AOT layer is unmodified even after addition of the polymer. Conversely, the polymer layer has an average scattering length density very close to that of pure polymer, with a molecular thickness comparable to that formed on the surface of pure water. Thus, it appears that the PDMS spreads on the AOT film with undetectable mixing of the two layers. Each layer retains its individual properties while separated by a small polymer–surfactant interface of 5 Å.

When the polymer concentrations are increased to amounts equivalent to 2 and 3 monolayers, curves 2b and 2c, respectively, are obtained. The same two-layer model is also found to describe these data very well (continuous lines). The parameters used to fit the data are for curve 2b, d_s = 13 Å and Nb = 0.90E-6 Å^{-2} (surfactant layer) and d_p = 15 Å and Nb = 3.98E-6 Å^{-2} (polymer layer) and for curve 2c, d_s = 13 Å and Nb = 0.90E-6 Å^{-2} (surfactant layer) and d_p = 28.5 Å and Nb = 3.07E-6 Å^{-2} (polymer layer). These results show that the scattering length density of the surfactant layer remains unchanged irrespective of the amount of polymer deposited on it, confirming the absence, or an undetectable amount, of mixing of AOT and PDMS.

Interpretation of the behavior of the polymer layer, however, is less straightforward. With an increase in polymer surface concentration, the average thickness of the polymer layer increases as expected, but the average scattering length density decreases. Such a decrease may be attributed to two possibilities: (i) presence of protonated surfactant or (ii) presence of air, in the polymer layer. One can determine without ambiguity whether it is one or the other (or both) by using deuterated surfactant, but in the absence of deuterated AOT, we can make some reasonable postulates. Since we have shown that under all circumstances there is no penetration of polymer into the surfactant layer, and the polymer–surfactant interface is small (5 Å), we propose that the probability of AOT molecules diffusing into the PDMS layer is minimal. The alternative, the presence of air in the polymer layer, would suggest a relatively inhomogeneous layer. In part 1 of our paper, we have shown that the surface of AOT acts as a poor solvent for PDMS in two dimensions. It is possible therefore that, on a molecular scale, the polymer film is inhomogeneous. At a macroscopic level, there is no clear indication of spreading problem up to these concentrations. At higher concentrations however, unspread regions of polymer are observed with Brewster angle microscopy (see Part I[18]). The existence of a spreading limit of the polymer on the modified surface results in partial spreading, giving rise to rather inhomogeneous polymer layers. For the concentrations studied here, the widths of the polymer–air interface are 5, 22, and 25 Å for 1, 2, and 3 monolayers, respectively. Note that at three monolayers, d_p is greater than 3 times the value of d_p at one monolayer, indicating that the polymer molecule adopts a less spread out conformation as the surface concentration is increased. This change in conformation coupled with the large polymer–air interface suggests that with increasing polymer concentration, the polymer layer becomes progressively less homogeneous. We note also that from the reflectivity data, the amounts of polymer deduced correspond to 84.3%, 77.5%, and 76.3% of the actual amounts deposited on the surface for 1, 2, and 3 monolayers, respectively. This apparent "loss" of polymer could arise

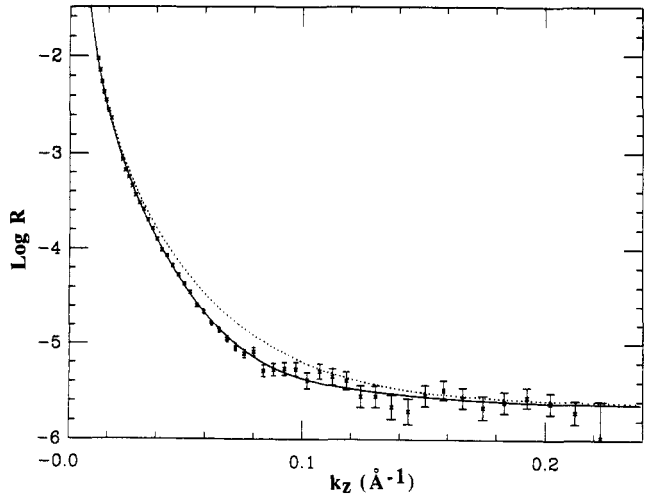

Figure 3. Reflectivity curve of $C_{10}E_5$ in D_2O. The dotted line is the Fresnel curve; the continuous line is calculated using a one-layer model: d_s = 18.5 Å, Nb = 0.85E-6 Å^{-2}.

from inhomogeneous spreading with some unspread domains collecting at the edge of the sample container outside the illuminated area of the surface.

The above data show clearly that when spread on the surface of a monolayer of AOT, PDMS does not penetrate the AOT to form a mixed polymer–surfactant layer. Rather, the PDMS forms a separate layer with the center of mass above that of the surfactant monolayer. This means that there is no favorable interaction of polymer and surfactant. The absence of polymer penetration into the surfactant layer also suggests the absence of polymer interaction with the water surface, since the surfactant layer presents a barrier between the polymer and the water surface. In our previous study of PDMS spread on the free surface of water,[10] we had explained the spread out two-dimensional conformation of the polymer to be favored by direct interaction of the slightly polar siloxane with water through hydrogen bonding. In the present case, in spite of the inaccessibility of the polymer to the water surface, we measure a thickness which corresponds to a spread two-dimensional conformation at 1 monolayer. It should be noted that films of very similar thickness (7 Å) have been observed on silanated wafers.[26] Hydrogen bonding as a mechanism for maintaining this conformation seems unlikely. In our case with AOT, even though the surfactant layer contains about 5% water, the water molecules are more likely to be situated near the charged headgroups than in the hydrocarbon chains, therefore even interaction of the polymer with these water molecules would require significant penetration into the surfactant layer. It is possible that the low cohesion energy of PDMS is sufficient to explain this spreading phenomenon even in the absence of strong monomer–substrate interaction. Another possibility is that when spread on the AOT monolayer, the PDMS molecule is not spread out with the siloxane backbone completely exposed but rather adopts a slightly helical conformation with a low energy. This helical structure has been proposed for PDMS spread on nonpolar liquids.[36,37]

In Figure 3, the reflectivity curve of the nonionic single chain surfactant, $C_{10}E_5$ (Nb = 0.16E-6 Å^{-2}) on D_2O is fitted to a one layer model with d_s = 18.5 Å and Nb = 0.85E-6 Å^{-2}, with an interface of 10 Å on each side of the layer. This gives $\phi_s = 0.89$ and $\phi_w = 0.11$. The nonionic surfactant thus solubilizes more water than AOT. For both AOT and $C_{10}E_5$, due to their low solubilities, the scattering length density of the water subphase is not modified.

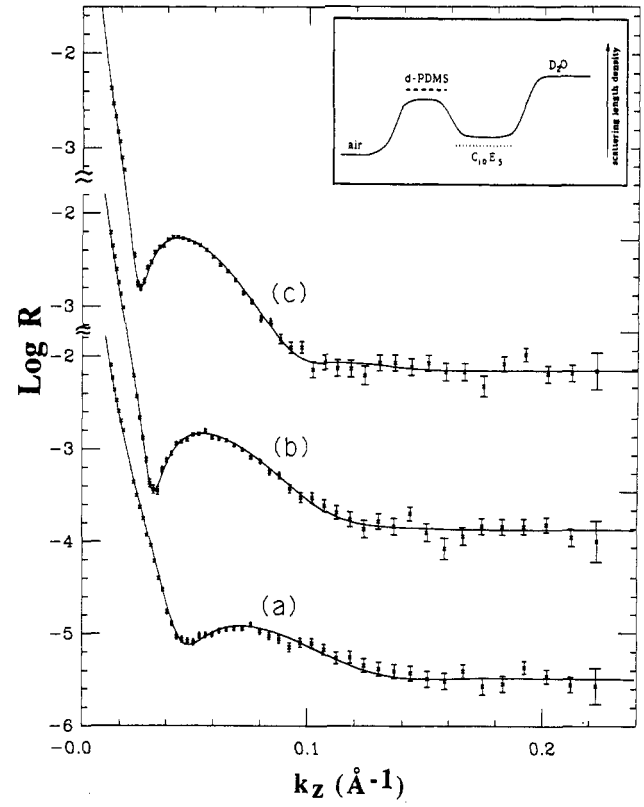

Figure 4. Reflectivity data for deuterated PDMS on the $C_{10}E_5$ monolayer with D_2O as the subphase at different polymer surface concentrations: 1.5 monolayers (a); 2.5 monolayers (b); 3.5 monolayers (c). The continuous lines are calculated using a two-layer model with the density profile shown in the inset (scattering length density for pure polymer (dashed line), for pure surfactant (dotted line)).

Parts a–c of Figure 4 show the reflectivity curves after addition of 1.5, 2.5, and 3.5 monolayers, respectively, of deuterated PDMS. As in previous figures, the continuous lines are calculated from two-layer models. Contrary to the case of AOT, we find in all cases a significant increase in the average scattering length density of the $C_{10}E_5$ layer (Nb = 1.85–2.15E-6 Å^{-2}) upon addition of the PDMS. This increase can be due to two possible reasons: (i) increased solubilization of deuterated water molecules in the surfactant layer upon addition of polymer and (ii) penetration of deuterated PDMS into the surfactant layer.

The problem of whether the scattering length density of the surfactant layer is increased by deuterated water or deuterated polymer can be resolved by using air contrast-matched water (average Nb = 0) as the subphase. In this case, the presence of water molecules in the surfactant layer would only serve to decrease the average scattering length density of the surfactant layer, and any increase observed can only be attributed to the deuterated polymer. Parts a–c of Figure 5 show the reflectivity curves corresponding to 1.5, 2.5, and 3.5 monolayers of deuterated PDMS spread on $C_{10}E_5$ in air contrast-matched water, together with calculated two-layer model curves (continuous lines). In all cases, the average scattering length density of the $C_{10}E_5$ layer is also found to be higher (Nb = 0.80–1.10E-6 Å^{-2}) than that expected for pure surfactant (0.16E-6 Å^{-2}). Since this increase cannot be due to presence of water molecules, we conclude unambiguously that there is penetration of the deuterated polymer into the surfactant layer. The data from the D_2O subphase and the air contrast-matched water subphase yield respectively the following equations: $\phi_s Nb_s + \phi_p Nb_p + \phi_w Nb_w = Nb_{D_2O}$ and $\phi_s Nb_s + \phi_p Nb_p + \phi_w Nb_w^0 = Nb_O$. Nb_w^0 is the average scattering length density of the air contrast-matched water

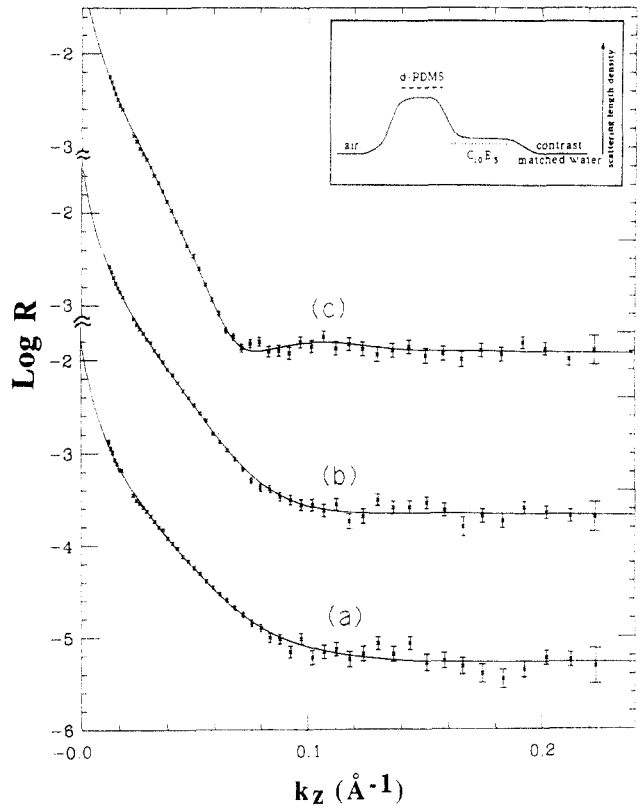

Figure 5. Reflectivity data for deuterated PDMS on the $C_{10}E_5$ monolayer with air contrast-matched water as the subphase at different polymer surface concentrations: 1.5 monolayers (a); 2.5 monolayers (b); 3.5 monolayers (c). The continuous lines are calculated using a two-layer model with the density profile shown in the inset (scattering length density for pure polymer (dashed line), for pure surfactant (dotted line)).

which is equal to zero, Nb_{D_2O} and Nb_O are the values obtained for the surfactant layer with D_2O and air contrast-matched water as the subphase, respectively. Coupled with mass balance $\phi_s + \phi_p + \phi_w = 1$, we have three equations from which we can deduce the composition of the surfactant layer in terms of the volume fraction of surfactant, polymer, and water, ϕ_s, ϕ_p, and ϕ_w, respectively. We obtain $\phi_s = 0.64$–0.70, $\phi_p = 0.14$–0.20, and $\phi_w = 0.16$–0.18. For each component, the range of values indicates the experimental dispersion between the two separate series of experiments. We find therefore, considerable penetration of PDMS into the $C_{10}E_5$ layer accompanied by a small increase in the amount of water in the surfactant layer. The width of the polymer–surfactant interface is 10 Å, larger than that of AOT–PDMS.

For the polymer-rich layer, the parameters obtained for 1.5, 2.5, and 3.5 monolayers are d_p = 10–12 Å, Nb_p = 3.20–3.60E-6 Å^{-2}; d_p = 18.5–19.8 Å, Nb = 3.95–4.15E-6 Å^{-2}; and d_p = 24–26 Å, Nb = 4.80–4.96E-6 Å^{-2}, respectively. At low surface concentration of the polymer, the average scattering length density of the polymer layer is lower than that of pure polymer (5.01E-6 Å^{-2}). With increasing amount of polymer added to the surface, the average scattering length density of the polymer layer increases and approaches that of pure polymer. This trend is opposite to that observed for the case of AOT–PDMS where the average scattering length density of the polymer layer decreases with concentration. A summary of these data is given in Table I. The error bars corresponding to a change in about 5% of the χ^2 values are as follows: for R_0, R_1, R_2 ±1 Å; for d_s, d_p ±0.2 Å; for Nb_s, Nb_p ±0.02E-6.

From the data of the surfactant-rich layer, we have shown that there is significant penetration of the polymer into the surfactant layer to form a mixed PDMS–$C_{10}E_5$ layer. This picture is consistent with our previous conclusion in part 1 that $C_{10}E_5$ acts as a good solvent for PDMS in two dimensions. As a result, at lower surface concentration of polymer, we do not obtain a pure polymer layer in the polymer-rich zone. Instead, this latter region seems to be only partially covered with polymer, with possibly some exposed ends of the surfactant chains. One can postulate that in this case, the PDMS molecule unfolds to interact with water molecules, as in the case when spread on the free surface of water. We can also surmise that penetration of PDMS into $C_{10}E_5$ is rendered more accessible by the greater flexibility of the film formed with the single-chain surfactant compared to that formed with the more rigid double-chain AOT.

With increasing polymer concentration, the polymer-rich layer becomes increasingly more saturated with pure polymer, as seen from the average scattering length density which approaches that of pure polymer at 3.5 monolayers. At 1.5, 2.5, and 3.5 monolayers of polymer, the average widths of the polymer–air interface are 8, 22, and 27 Å, respectively. Thus, even though the values of the polymer film thickness suggest that the polymer molecules adopt a flat two-dimensional conformation with respect to its three-dimensional coil, the increase in the width of the polymer–air interface indicates a decrease in the extent of spreading with increasing amount of polymer. Macroscopically, no inhomogeneity is observed up to these concentrations. For all the three concentrations of polymer spread on $C_{10}E_5$, the amounts of polymer deduced from the reflectivity data correspond to more than 95% of the actual amounts deposited on the surface.

In the above studies, we have shown that PDMS spreads out to form a two-dimensional molecularly thin film on the surface of pure water as well as on the surface of water covered with a monolayer of surfactant. Such a surface oriented conformation is entropically unfavorable unless balanced by an interaction energy. In our case, we spread the PDMS from a spreading solvent in which the PDMS adopts a random coil conformation. Upon evaporation of the spreading solvent, the polymer molecule, which now sits on the surface, can retain its original three-dimensional random coil or it can take on a flat film structure of molecular thickness. Such a change from three-dimensional to two-dimensional conformation involves a loss in configuration entropy which must be overcome by energy of monomer–substrate interaction. (It may also adopt intermediate conformations such as the proposed helical conformation,[36,37] but we will consider here only the two extreme cases of three-dimensional random coil and two-dimensional flat film.) For a polymer molecule with one point fixed on the surface, the entropy of the molecule depends on the total number of possible configurations,[38] $\Gamma(N) = z^N$, where N is the number of monomers and z is the coordination number. If we take a simple lattice model, z is 6 in three dimensions and 4 in two dimensions. Therefore, in going from a three-dimensional to a two-dimensional conformation, the change in configurational entropy is $\ln 4^N - \ln 6^N = N \ln(4/6)$ or $-0.405N$ (in k_B units). Note that entropic loss is directly proportional to the chain length. This explains why entropically it is less favorable for longer chain molecules to adopt a confined structure such as that of an adsorbed, a flattened, or a stretched conformation unless this loss is entropic energy is overcome by an interaction energy. In our case of PDMS on surfactant, we have no measure of the monomer–surfactant interaction but the fact that PDMS spreads indicates that the energy of such interaction overcomes

Table I. Summary of Neutron Reflectivity Data[a]

C_p (monolayer)	R_0 (Å)	d_s (Å)	$10^6 Nb_s$ (Å^{-2})	R_1 (Å)	d_p (Å)	$10^6 Nb_p$ (Å^{-2})	R_2 (Å)
AOT (D_2O Subphase)							
AOT only	9	13	0.90	5			
1.0	9	13	0.90	5	6.5	4.95	5
2.0	13	13	0.90	5	15.0	3.98	22
3.0	9	13	0.90	5	28.5	3.07	25
$C_{10}E_5$ (D_2O Subphase)							
$C_{10}E_5$ only	10	18.5	0.85	10			
1.5	12	18.5	2.15	10	12.0	3.20	8
2.5	10	18.5	1.85	10	19.8	3.95	20
3.5	11	18.5	2.05	10	26.0	4.96	26
$C_{10}E_5$ (Air Contrast-Matched Water Subphase)							
1.5	10	18.5	1.10	10	10	3.60	8
2.5	10	18.5	0.80	10	18.5	4.15	24
3.5	10	18.5	0.90	10	24.0	4.80	28

[a] C_p is the polymer surface concentration (expressed in the number of monolayers), R_0, R_1, and R_2 are the interfacial widths of surfactant–water, surfactant–polymer (or air), and polymer–air, d_s and d_p are the thicknesses of the surfactant and polymer layers, and Nb_s and Nb_p are the average scattering length densities of the surfactant and polymer layers, respectively.

the entropic loss. On the surface of pure water, H bonding energy between the exposed siloxane oxygen and the water molecule certainly exceeds such entropic loss.

The spreading capacity of PDMS on both hydrophilic and hydrophobic surfaces to form molecularly thin films can also be understood in terms of its low intermolecular forces or cohesive energy. This is manifested in its low glass transition temperature (T_g = −120 °C[39]), low temperature dependence of its viscosity, and high compressibility. Another direct manifestation of the cohesive energy is the surface tension. These two properties are related by an empirical expression[40] $\gamma \approx 0.75 e_{coh}^{2/3}$, where γ is the surface tension and e_{coh} is the cohesive energy density. The surface tension of PDMS, γ_{PDMS}, is about 19–20 dyne/cm. Such a low surface tension value results in a positive spreading parameter $S = \gamma_S - \gamma_{PDMS} - \gamma_{S/PDMS}$ for many substrates, allowing spontaneous spreading of the PDMS. γ_S is the surface tension of the substrate, and $\gamma_{S/PDMS}$, the interfacial tension between the substrate and PDMS. As can be seen from the expression of the spreading parameter, the interfacial tension also plays an important role in the spreading process. One can estimate the interfacial tension between two materials 1 and 2 by the general expression given by Owens and Wendt:[41] $\gamma_{12} = \gamma_1 + \gamma_2 - 2(\gamma_1^d\gamma_2^d)^{1/2} - 2(\gamma_1^h\gamma_2^h)^{1/2}$, where $\gamma = \gamma^d + \gamma^h$ and the superscripts d and h refer to dispersion and hydrogen bonding force components, respectively. For PDMS,[41,42] in units of dyne/cm, γ_{PDMS}^d = 16.9 and γ_{PDMS}^h = 2.1. For the surface of water covered with a saturated layer of AOT, γ_S = 28.5.[18] If we assume that the contribution from the hydrogen bonding force is negligible on the AOT layer (γ^h = 0), we obtain an interfacial tension $\gamma_{AOT/PDMS}$ = 3.6, giving a corresponding value of about +5.9 for S (using γ_{PDMS} = 19). For the surface of water covered with $C_{10}E_5$, γ_S = 31.5;[18] $\gamma_{C_{10}E_5/PDMS}$ = 4.4, giving a corresponding S value of +8.1, higher than that for AOT. These values show that PDMS can spread spontaneously on the AOT and $C_{10}E_5$ covered water surfaces, as observed experimentally. Note that these estimations assume negligible contribution from hydrogen bonding forces. For the case of AOT where the double chain hydrocarbon tails are rather closely packed, this assumption may be justified by the fact that γ^h = 0 for alkanes. For the case of $C_{10}E_5$ where there is some degree of water molecules incorporated in the surfactant film, γ^h may not be negligible; in this case, we would obtain a lower value for the interfacial tension and an even higher positive value of S.

Summary

This work shows clearly that at the water–air interface, mixed surfactant–PDMS layers are a superposition of two layers: a surfactant-rich and a polymer-rich layer. The composition, and therefore the degree of mixing of the components in each layer, depend strongly on the nature of the surfactant. We measure significant penetration of PDMS into the $C_{10}E_5$ layer (14–20%). In the case of AOT, no interpenetration of the two layers is detected and the interface of the layers is sharper (5 Å compared to 10 Å for $C_{10}E_5$). The polymer layer on AOT seems to incorporate air, the amount of which increases with polymer concentration, suggesting an increasing degree of inhomogeneity. This is in agreement with ellipsometry data and Brewster angle microscopy images discussed in part 1 of our paper. The wetting behavior of PDMS is markedly different on the two surfaces; our study of the two model systems shows that it is strongly related to the degree of interpenetration of the polymer and the surfactant layers.

The results of surfactant layers in the absence of polymer show that the AOT layer contains about 5% water while the $C_{10}E_5$ layer contains about 11% water. AOT is a double-chain anionic surfactant which forms relatively compact layers. $C_{10}E_5$ on the other hand is a single-chain nonionic surfactant and forms monolayers in which the area per chain ~40 Å^2 is about twice the minimum value for hydrocarbon chains. It is therefore expected that the $C_{10}E_5$ layer will be more flexible than that of AOT. This has been confirmed by the values of the bending elastic moduli of monolayers of AOT[43] and nonionic surfactants[44] similar to $C_{10}E_5$. The significant penetration of PDMS into $C_{10}E_5$ compared to AOT could be due to either the larger flexibility or/and to the higher water content in the $C_{10}E_5$ layer.

Polymer spreading is controlled by a competition of monomer–monomer and monomer–substrate interactions. The latter must overcome the entropy loss as a result of uncoiling of the molecule from a three-dimensional random coil to a flat two-dimensional conformation. This entropic factor is obviously unfavorable for polymer penetration into the surfactant layer and may explain the behavior of alkane penetration into surfactant layers, which is, as mentioned earlier, limited to short chain alkanes. Since at low concentrations the polymer spreads out on the surface, the entropy term is clearly negligible in this case compared to the molecular interactions. Our result is likely to be also relevant to the problem of polymer solubilization in microemulsions. It is generally agreed that the polymer is solubilized in the core of the microemulsion droplet if the core size is larger than the radius of the polymer coil; this would not be the case if the molecular interactions of monomers and surfactants are large enough to produce a flat polymer conformation along the droplet surface, or even penetration of the polymer into the surfactant layer.

Acknowledgment. We thank A. Lapp for the generous gift of the deuterated polymers. L.T.L. is very appreciative of fruitful discussions with M. Daoud. The comments and suggestions of one of the referees have been very helpful in bringing out more clearly the information and ideas presented in this paper.

References and Notes

(1) Gaines, G. L. *Insoluble Monolayers at Liquid-Gas Interfaces*; Wiley: New York, 1966.

(2) Gaines, G. L., Jr. *Langmuir* **1991**, *7*, 834.
(3) Granick, S. *Macromolecules* **1985**, *18*, 1597.
(4) Vilanove, R.; Poupinet, D.; Rondelez, F. *Macromolecules* **1988**, *21*, 2880.
(5) Kawaguchi, M.; Tohyama, M.; Mutoh, Y.; Takahashi, A. *Langmuir* **1988**, *4*, 407.
(6) Kawaguchi, M.; Tohyama, M.; Takahashi, A. *Langmuir* **1988**, *4*, 411.
(7) Sauer, B. B.; Yu, H.; Yazdanian, M.; Zografi, G.; Kim, M. W. *Macromolecules* **1989**, *22*, 2332.
(8) Kawaguchi, M.; Sauer, B. B.; Yu, H. *Macromolecules* **1989**, *22*, 1735.
(9) Mann, E. K.; Langevin, D. *Langmuir* **1991**, *7*, 1112.
(10) Lee, L. T.; Mann, E. K.; Langevin, D.; Farnoux, B. *Langmuir* **1991**, *7*, 3076.
(11) Henderson, J. A.; Richards, R. W.; Penfold, J.; Shackleton, C.; Thomas, R. *Polymer* **1991**, *32*, 3284.
(12) Brinkhuis, R. H. G.; Schouten, A. J. *Macromolecules* **1991**, *24*, 1487.
(13) Noll, W.; Steinbach, H.; Sucker, C. *Ber. Bunsen-Ges. Phys. Chem.* **1963**, *67*, 407.
(14) Gruen, D. W. R.; Haydon, D. A. *Biophys. J.* **1981**, *33*, 167.
(15) Hoffmann, H.; Ulbricht, W. *J. Colloid Interface Sci.* **1989**, *129*, 388.
(16) Binks, B. P.; Kellay, H.; Meunier, J. *Europhys. Lett.* **1991**, *16*, 53.
(17) Lee, J. R.; Thomas, R. K.; Aveyard, R.; Binks, B. P.; Cooper, P.; Flechter, P. D. I.; Sokolowski, A.; Penfold, J. *J. Phys. Chem.* **1992**, *96*, 10971.
(18) Mann, E.; Lee, L. T.; Hénon, S.; Langevin, D. Meunier, J. Preceding article in this issue.
(19) Werner, S. A.; Klein, A. G. In *Neutron Scattering*; Skold, K., Price, D. L., Eds.; Academic: New York, 1986.
(20) Penfold, J.; Thomas, R. *J. Phys. Condens. Matter* **1990**, *2*, 1369.
(21) Born, M.; Wolf, E. *Principles of Optics*; Pergamon Press: Oxford, U.K., 1975.
(22) Sinha, S. K.; Sirota, E. B.; Garoff, S.; Stanley, H. B. *Phys. Rev. B* **1988**, *38*, 2297.
(23) Braslau, A.; Pershan, P. S.; Swislow, G.; Ocko, B. M.; Als-Nielsen, J. *Phys. Rev. A* **1988**, *38*, 2457.
(24) Schwartz, D. K.; Schlossman, M. L.; Kawamoto, E. H.; Kellogg, G. J.; Pershan, P. S.; Ocko, B. M. *Phys. Rev. A* **1990**, *41*, 5687.
(25) Sanyal, M. K.; Sinha, S. K.; Huang, K. G.; Ocko, B. M. *Phys. Rev. Lett.* **1991**, *66*, 628.
(26) Daillant, J.; Benattar, J. J.; Leger, L. *Phys. Rev. A* **1990**, *41*, 1963.
(27) Parratt, L. G. *Phys. Rev.* **1954**, *95*, 359.
(28) Lekner, J. *Theory of Reflection*; Martinus Nijhoff: Dordrecht, The Netherlands, 1987.
(29) Bradley, J. E.; Lee, E. M.; Thomas, R. K.; Willatt, A. J.; Penfold, J.; Ward, R. C.; Gregory, D. P.; Waschkowski, W. *Langmuir* **1988**, *4*, 821.
(30) Lee, E. M.; Thomas, R. K.; Penfold, J.; Ward, R. C. *J. Phys. Chem.* **1989**, *93*, 381.
(31) Rennie, A. R.; Crawford, R. J.; Lee, E. M.; Thomas, R. K.; Crowley, T. L.; Roberts, S.; Qureshi, M. S.; Richards, R. W. *Macromolecules* **1989**, *22*, 3466.
(32) Satija, S. K.; Majkrzak, C. F.; Russell, T. P.; Sinha, S. K.; Sirota, E. B.; Hughes, G. J. *Macromolecules* **1990**, *23*, 3860.
(33) Guiselin, O.; Lee, L. T.; Farnoux, B.; Lapp, A. *J. Chem. Phys.* **1991**, *95*, 4632.
(34) Grundy, M. J.; Richardson, R. M.; Roser, S. J.; Penfold, J.; Ward, R. C. *Thin Solid Films* **1988**, *159*, 43.
(35) Vilanove, R.; Rondelez, F. *Phys. Rev. Lett.* **1980**, *45*, 1502.
(36) Jarvis, N. L. *J. Colloid Interface Sci.* **1969**, *29*, 647.
(37) Noll, W. *Chemistry and Technology of Silicones*; Academic Press: London, 1968.
(38) de Gennes, P. G. *Scaling Concepts in Polymer Physics*; Cornell University Press: Ithaca, NY, 1979.
(39) Brandrup, J.; Immergut, E. H. *Polymer Handbook*, 2nd ed.; Wiley: New York, 1974.
(40) Van Krevelen, D. W. *Properties of Polymers*; Elsevier: Amsterdam, 1976.
(41) Owens, D. K.; Wendt, R. C. *J. Appl. Polym. Sci.* **1969**, *13*, 1741.
(42) Fowkes, F. M. *Ind. Eng. Chem.* **1964**, *56*, 40.
(43) Binks, B. P.; Meunier, J.; Abillon, O.; Langevin, D. *Langmuir* **1989**, *5*, 415.
(44) Lee, L. T.; Langevin, D.; Meunier, J.; Wong, K.; Cabane, B. *Prog. Colloid Polym. Sci.* **1990**, *81*, 201.